

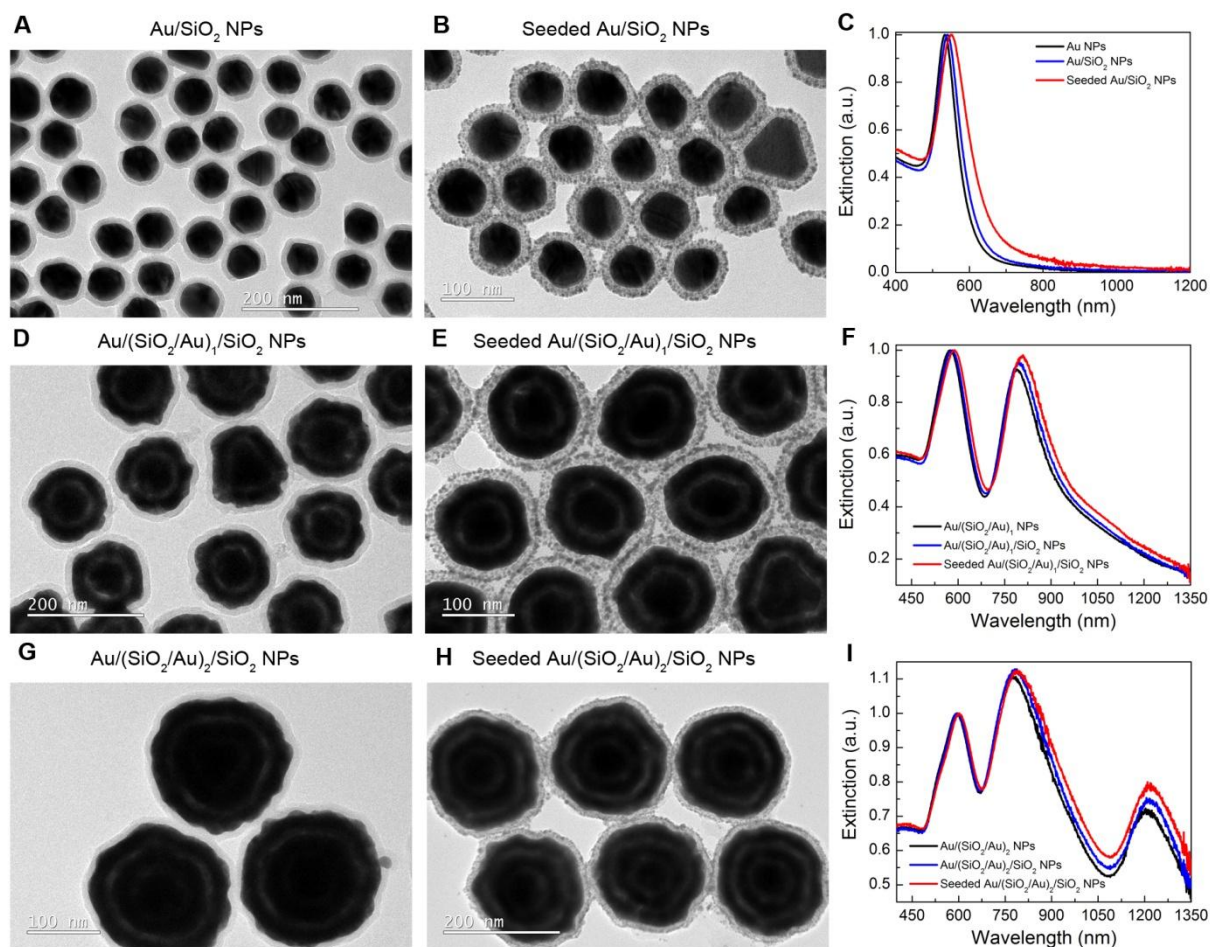
## Supporting Information

**Metaparticles: dressing nano-objects with a hyperbolic coating**

*Pan Wang\**, *Alexey V. Krasavin*, *Francesco N. Viscomi*, *Ali M. Adawi*, *Jean-Sebastien Bouillard*, *Lei Zhang*, *Diane J. Roth*, *Limin Tong*, *Anatoly V. Zayats\**

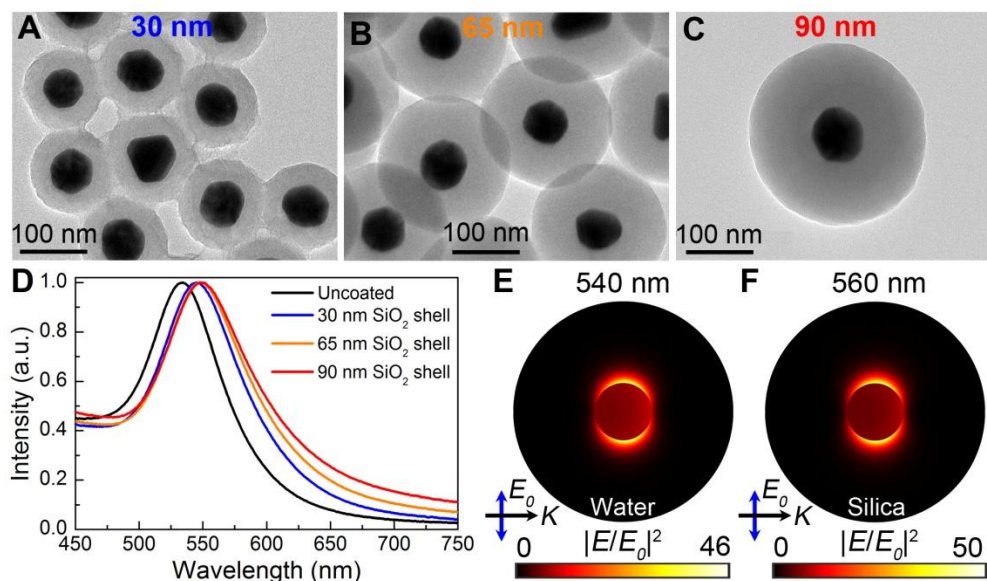
**Section 1. Additional TEM images and extinction spectra**

Figure S1 presents TEM images of nanoparticles obtained at intermediate stages of the multishell coating process, as well as the corresponding extinction spectra. The thickness of the SiO<sub>2</sub> shells is ~10 nm (Figure S1A,D,G), small Au seeds can be seen clearly from the images shown in Figure S1B,E,H. The resonance peaks experience gradual red shift after the coating of SiO<sub>2</sub> shells and Au seeds (Figure S1C,F,I).



**Figure S1.** (A,B) TEM images of Au/SiO<sub>2</sub> and seeded Au/SiO<sub>2</sub> nanoparticles. (C) Corresponding extinction spectra in water. (D,E) TEM images of Au/(SiO<sub>2</sub>/Au)<sub>1</sub>/SiO<sub>2</sub> and seeded Au/(SiO<sub>2</sub>/Au)<sub>1</sub>/SiO<sub>2</sub> nanoparticles. (F) Corresponding extinction spectra in water. (G,H) TEM images of Au/(SiO<sub>2</sub>/Au)<sub>2</sub>/SiO<sub>2</sub> and seeded Au/(SiO<sub>2</sub>/Au)<sub>2</sub>/SiO<sub>2</sub> nanoparticles. (I) Corresponding extinction spectra in water. Subscript n in (SiO<sub>2</sub>/Au)<sub>n</sub> indicates the number of SiO<sub>2</sub>/Au bishells.

## Section 2. Optical properties of SiO<sub>2</sub> coated Au nanospheres



**Figure S2.** (A–C) TEM images of Au nanospheres (~62 nm in diameter) coated with 30, 65 and 90 nm SiO<sub>2</sub> shells, respectively. (D) Extinction spectra of uncoated and SiO<sub>2</sub> coated Au nanospheres measured in water. (E,F) Electric field distributions for an uncoated Au nanosphere in water (E) and an Au nanosphere coated with a 90-nm SiO<sub>2</sub> shell (F) plotted at the wavelengths corresponding to the resonance peaks.

## Section 3. Absorption spectrum of SH-PEG molecules

To measure the absorption spectrum of SH-PEG molecules, 5 mg of SH-PEG powder was dissolved in 5 mL of CHCl<sub>3</sub> (concentration ~0.2 μM). By comparing the absorption spectra of pure CHCl<sub>3</sub> solvent and the SH-PEG solution, one can obtain the absorption spectrum of HS-PEG molecules, as shown in Figure S3, absorption peaks can be easily seen in the infrared wavelength range, which match the peaks in Figure 3C in the main text.

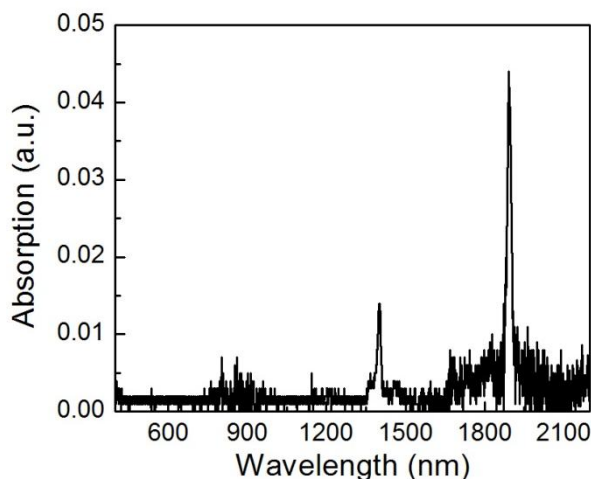


**Figure S3.** Absorption spectrum of HS-PEG molecules: two sharp peaks can be clearly seen.

#### **Section 4. Scattering spectra of single metaparticles**

Scattering spectra of single metaparticles were measured in the total internal reflection geometry, as shown schematically in Figure S4A. Briefly, a droplet of metaparticle solution was first spin-coated onto a coverslip, which was brought into contact with the surface of a hemicylindrical prism using immersion oil. Then, white light from a halogen lamp was focused onto the coverslip at an incident angle of  $60^\circ$ , which can excite the metaparticles on the coverslip by the evanescent field. Finally, the scattering from the metaparticles was collected by a 50X objective lens ( $NA = 0.42$ ) and directed to a charge-coupled device camera for imaging and a spectrometer (Triax 332, Horiba Jobin Yvon) for a spectral analysis. The measured scattering spectra were calibrated by the spectrum of the white light. The scattering spectra of the metaparticles with one, two and three pairs of  $\text{SiO}_2/\text{Au}$  shells and corresponding dark-field scattering images of single metaparticles are shown in Figure S4B–D.

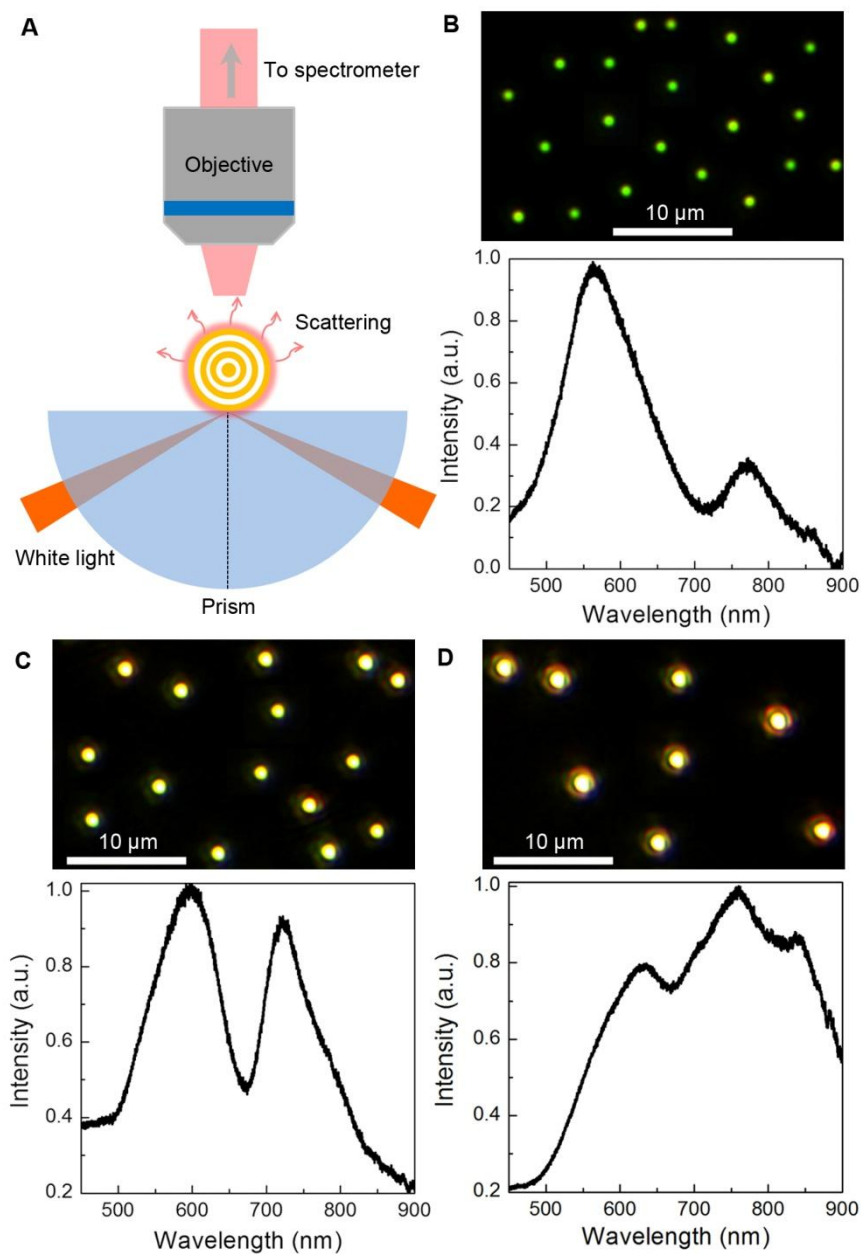


**Figure S4.** (A) Schematic illustration of the setup for light scattering imaging and spectroscopy of single metaparticles. (B–D) Dark-field scattering images and corresponding scattering spectra of single metaparticles with one (B), two (C) and three (D) pairs of SiO<sub>2</sub>/Au shells.

## Section 5. Refractive index sensitivity measurement

To evaluate the sensitivity of plasmonic resonances of metaparticles to the refractive index of their surroundings, the extinction spectra of metaparticles with three pairs of SiO<sub>2</sub>/Au shells dispersed in water, ethanol, and chloroform were measured. As shown in Figure S5A, all of the plasmonic resonances of the metaparticles red-shift when the solvent is changed from water (refractive index 1.333) to chloroform (refractive index 1.445). By measuring the respective resonance positions, one can estimate the refractive index sensitivities for each resonance (Figure S5B–E). The refractive index sensitivity of peak 4 reaches a value as high as 740 nm/RIU (refractive index unit), which is much higher than that of uncoated Au nanospheres (~120 nm/RIU, obtained from Figure S2) or Au nanoshells (~300 nm/RIU) [31].

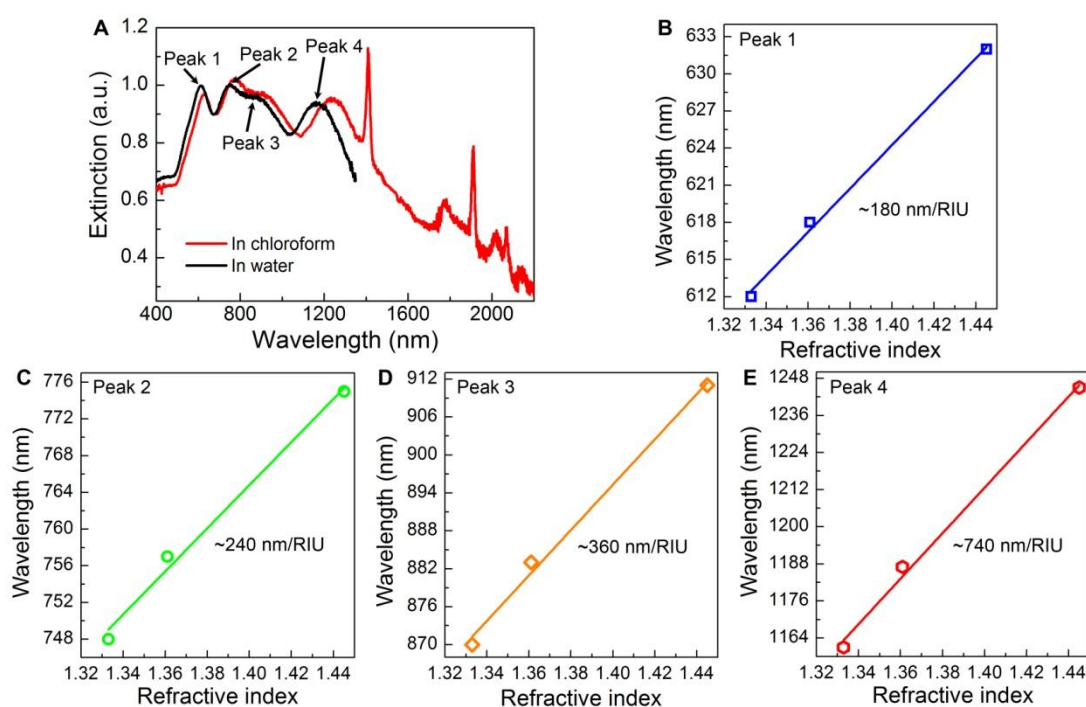


**Figure S5.** (A) Extinction spectra of metaparticles with three pairs of SiO<sub>2</sub>/Au shells measured in water (black curve) and chloroform (red curve). (B–E) Dependence of the resonance positions (indicated in A) on the refractive index of the surrounding solvent.

## Section 6. Spectral tuning of metaparticles

The optical properties of metaparticles can also be tuned by the control of the thickness of the outermost Au shell. Figure S6 shows the example of tuning the extinction spectra of the metaparticles with two and three pairs of SiO<sub>2</sub>/Au shells by changing the thickness of the outermost Au shell. With the increasing thickness, the resonances experience a blue shift, with longer wavelength resonances moving faster than short-wavelength ones.

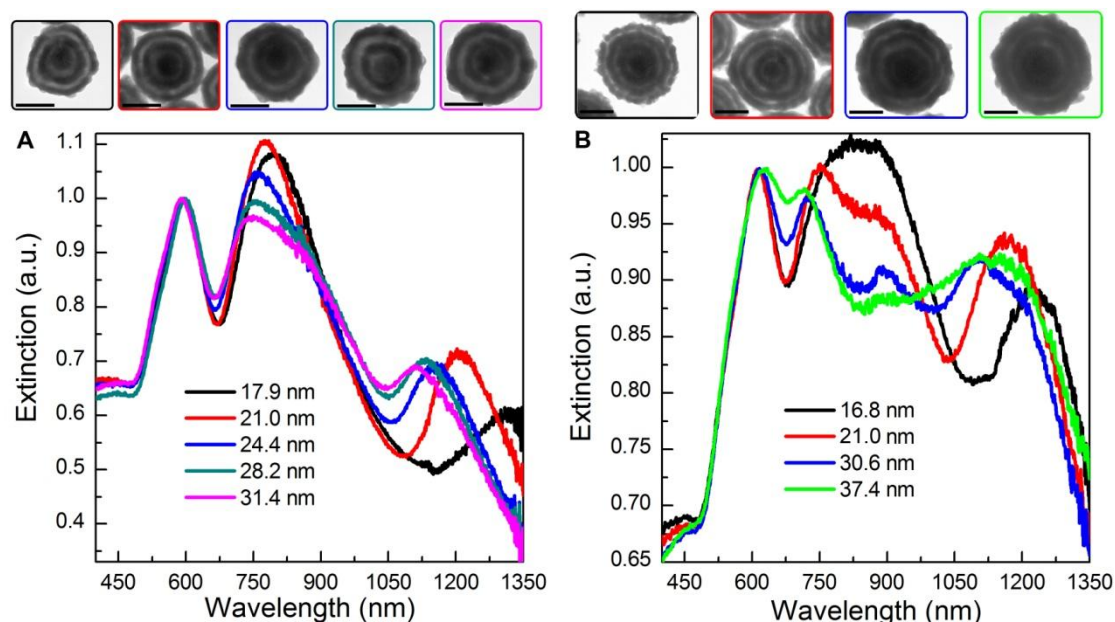


**Figure S6.** (A) Extinction spectra of metaparticles with two pairs of SiO<sub>2</sub>/Au shells with various outermost Au shell thicknesses measured in water. Inset: corresponding TEM images of the metaparticles with average outermost Au shell thicknesses of (from left to right) 17.9, 21.0, 24.4, 28.2, and 31.4 nm, respectively. (B) Extinction spectra of metaparticles with three pairs of SiO<sub>2</sub>/Au shells with various outermost Au shell thicknesses measured in water. Inset: corresponding TEM images of the metaparticles with average outermost Au shell thicknesses of (from left to right) 16.8, 21.0, 30.6, and 37.4 nm, respectively.

## Section 7. Optical properties of Au nanospheres with homogeneous hyperbolic coating

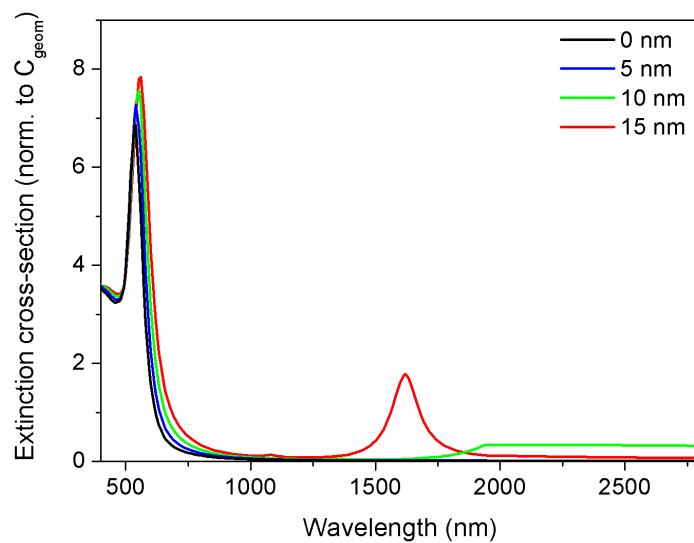


**Figure S7.** Evolution of the calculated extinction cross-section (normalized to the corresponding geometrical cross-section) of Au nanospheres with the decrease of the thickness of the uniform hyperbolic coating with permittivity shown in Figure 4A.

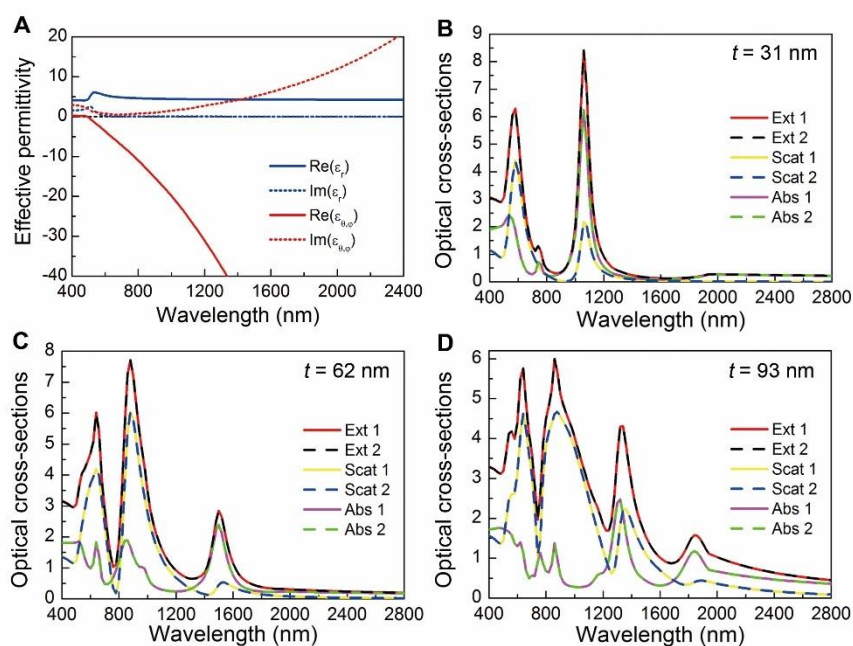


**Figure S8.** A) Effective permittivity determined using the EMT of SiO<sub>2</sub>/Au multishells with  $f_{Au}$  of 0.5 ( $t_{SiO_2} = 10$  nm,  $t_{Au} = 10$  nm). B–D) Numerical simulation results: calculated optical (absorption, scattering and extinction) cross-sections, normalized to the corresponding geometrical cross-sections ( $C_{geom} = \pi(r + t)^2$ ), of Au nanospheres with a homogeneous hyperbolic coating layer with permittivity shown in (A) for coating thicknesses ( $t$ ): 31 nm (B), 62 nm (C) and 93 nm (D).

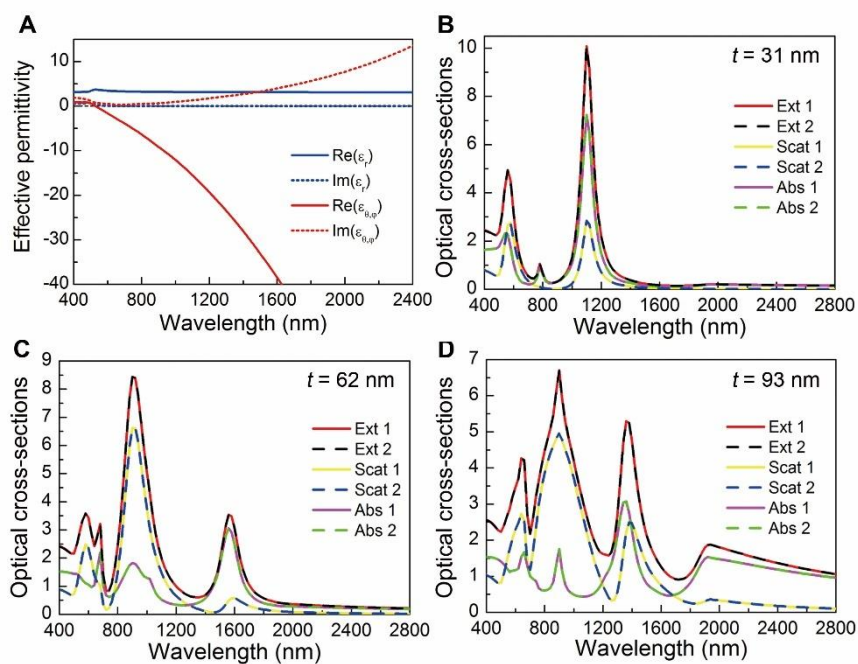


**Figure S9.** A) Effective permittivity determined using the EMT of SiO<sub>2</sub>/Au multishells with  $f_{Au}$  of 0.32 ( $t_{SiO_2} = 21$  nm,  $t_{Au} = 10$  nm). B–D) Numerical simulation results: calculated optical (absorption, scattering and extinction) cross-sections, normalized to the corresponding geometrical cross-sections ( $C_{geom} = \pi(r + t)^2$ ), of Au nanospheres with a homogeneous hyperbolic coating layer with permittivity shown in (A) for coating thicknesses ( $t$ ): 31 nm (B), 62 nm (C) and 93 nm (D).

## Section 8. Optical properties of silica nanospheres with hyperbolic coating

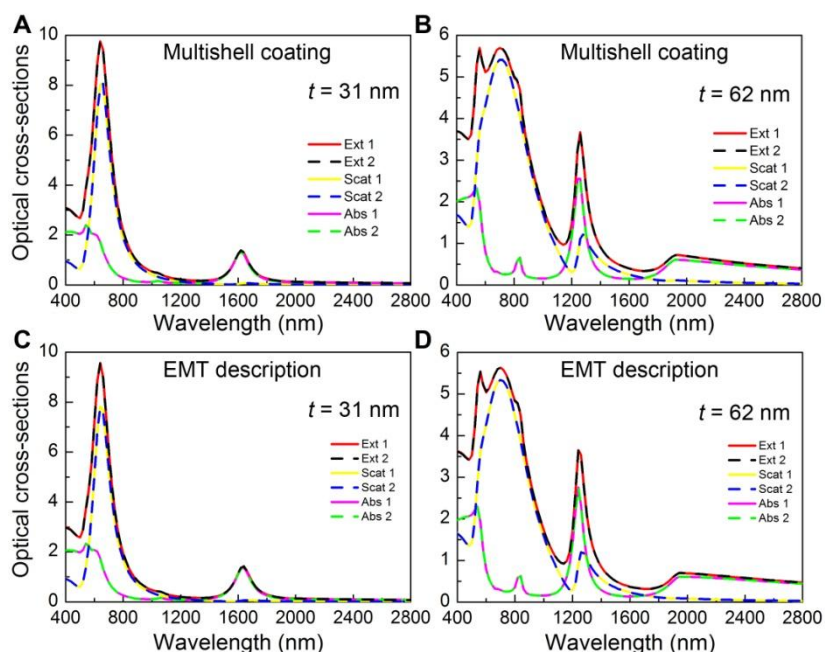


**Figure S10.** (A,B) Calculated optical (absorption, scattering and extinction) cross-sections, normalized to the corresponding geometrical cross-sections ( $C_{geom} = \pi(r + t)^2$ ), of  $\text{SiO}_2$  nanospheres ( $r = 31$  nm) with four (A) and eight (B) pairs of  $\text{SiO}_2/\text{Au}$  shells ( $t_{\text{SiO}_2} = 2.5$  nm,  $t_{\text{Au}} = 5.25$  nm), respectively. (C,D) Calculated optical (absorption, scattering and extinction) cross-sections, normalized to the corresponding geometrical cross-sections ( $C_{geom} = \pi(r + t)^2$ ), of silica nanospheres ( $r = 31$  nm) with a homogeneous hyperbolic coating layer with permittivity shown in Figure 4A for coating thicknesses ( $t$ ): 31 nm (C) and 62 nm (D), respectively.

## Section 9. Active metaparticles

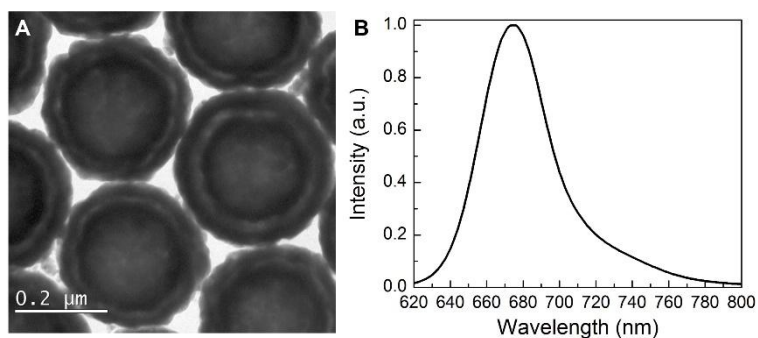


**Figure S11.** A) TEM image of dye-doped polystyrene nanoparticles coated with Au/SiO<sub>2</sub>/Au shells. The average diameter of polystyrene nanoparticles is ~220 nm. B) Emission spectrum of single active metaparticles excited at a 532-nm wavelength.

## Section 10. Examples of self-assembled metaparticles

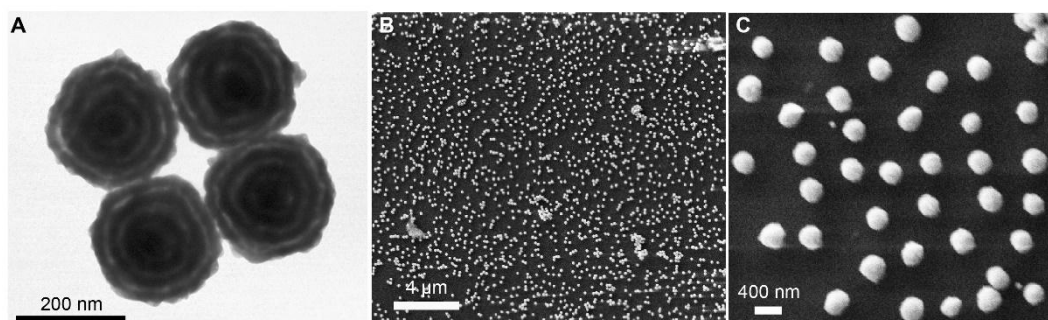


**Figure S12.** A) TEM image of four coupled metaparticles with three pairs of SiO<sub>2</sub>/Au shells. B) SEM image of a monolayer of metaparticles with three pairs of SiO<sub>2</sub>/Au shells self-assembled on a glass slide. C) An enlarged view of the monolayer.